# Data-driven modeling of equatorial atmospheric waves: the role of moisture and nonlinearity on global-scale instabilities and propagation speeds

Andre S. W. Teruya,[1, a)] Breno Raphaldini,[2] Carlos F. M. Raupp,[1] Pedro S. Peixoto,[3] Victor C. Mayta,[4] and Pedro L. Silva-Dias[1]

[1)]*Instituto de Astronomia, Geofísica e Ciências Atmosféricas, Universidade de São Paulo, 05508-090 Sao Paulo, Brazil.*

[2)]*High Altitude Observatory, NSF National Center for Atmospheric Research, 80301 Boulder, Colorado, USA.*

[3)]*Departamento de Matemática Aplicada, Instituto de Matemática e Estatística, Universidade de São Paulo, 05508-090 Sao Paulo, Brazil.*

[4)]*Department of Atmospheric Sciences, University of Wisconsin, 53706 Madison, Wisconsin, USA.*

(Dated: 23 April 2024)

Chaos
An Interdisciplinary Journal
of Nonlinear Science





Data-driven modeling of equatorial atmospheric waves

The equatorial region of Earth's atmosphere serves as both a significant locus for phenomena, including the Madden-Julian Oscillation (MJO), and a source of formidable complexity. This complexity arises from the intricate interplay between nonlinearity and thermodynamic processes, particularly those involving moisture. In this study, we employ a normal mode decomposition of atmospheric reanalysis ERA-5 datasets to investigate the influence of nonlinearity and moisture on amplitude growth, propagation speed, and mode coupling associated with equatorially trapped waves. We focus our analysis on global-scale baroclinic Kelvin and Rossby waves, recognized as crucial components contributing to the variability of the MJO. We examine the dependence of wave amplitudes on the background moisture field in the equatorial region, as measured by total column water vapor. Our analysis demonstrates the crucial role of moisture in exciting these waves. We further investigate the dependence of the propagation speed of the waves on their amplitudes and the background moisture field. Our analysis reveals a robust correlation between the phase speed of the normal modes and their corresponding amplitude, whereas a weaker correlation is found between the eigenmodes' phase speed and the moisture field. Hence, our findings suggest that moisture plays a role in exciting the global-scale Rossby-Kelvin structure of the MJO. In this context, the propagation speed of the eigenmodes is mainly influenced by their amplitudes, underscoring the significant role of nonlinearity in the wave propagation.

[a)]Corresponding author's address: Rua do Matão, 1226, 05508-090, Sao Paulo, Sao Paulo, Brazil. E-mail: andre.teruya@usp.br

Chaos
An Interdisciplinary Journal
of Nonlinear Science







## I. SUMMARY

**The Madden-Julian Oscillation (MJO) is the dominant variability mode of the tropical atmosphere on intraseasonal timescales (20-90 days), being responsible for important weather and climate impacts all over the Globe. The spatial structure of the MJO at planetary-scales exhibits a symmetric vortical structure about the equatorial plane due to the activity of equatorial Rossby waves, as well as a zonal jet structure centered at the equator due to the Kelvin wave activity. However, the MJO propagation speed no longer matches that of either Rossby or Kelvin waves, implying that the phase speed of these modes can be significantly modified during the MJO life cycle. Here, we use atmospheric (reanalysis) datasets combined with systematic decomposition techniques in order to gain insight into the physical mechanisms that can modify the dynamics of the planetary-scale Rossby and Kelvin waves during the onset of a MJO event.**

## II. INTRODUCTION

The equatorial region of the Earth's atmosphere is a place where important phenomena such as the El Niño Southern Oscillation[1], the Madden-Julian Oscillation[2] and the quasi-biennial oscillation[3] occur. In terms of its dynamics, the tropical atmosphere presents formidable complexity for several reasons: (i) the vanishing vertical component of the Coriolis force at the equator leads to the emergence of equatorially trapped wave modes confined within the tropical belt[4]; (ii) thermodynamic processes linked to moist convection and air-sea interactions play substantial roles in the atmospheric dynamics within this region of the globe[5–8]; (iii) nonlinear processes such as nonlinear interaction between different wave types lead to the coupling between distinct timescales, and possibly to chaotic dynamics[8–11]. A comprehensive review of the interplay between nonlinearity, moist convection, and equatorial wave dynamics is presented in Khouider, Majda, and Stechmann [12].

The theory of equatorial waves serves as a foundational element for comprehending tropical dynamics. Beginning with the seminal works of Matsuno [13] and Gill [14], the existence of equatorially trapped waves was conjectured based on theoretical grounds. Subsequently, the existence of equatorially trapped waves that have no mid-latitude analogs such as Kelvin and mixed Rossby-gravity modes, as well equatorial Rossby and inertio-gravity modes, was confirmed in observa-

tional studies[15–18]. A critical aspect of equatorial wave dynamics involves the observation that the signatures of these waves in wavenumber-frequency spectra[16] result in propagation speeds significantly slower than anticipated by dry linear theory. This phenomenon suggests that the coupling with moist convection is accountable for the reduction in the propagation speed of these waves[6]. On the other hand, when the feedback of the wave dynamics on the moisture transport is considered, apart from the convectively coupled waves, there emerges another eigenmode, which has been labeled as *moisture mode*[19–21]. Consequently, several theories have been proposed to elucidate the observed equatorial wave spectra in the context of linear equatorial wave dynamics in the presence of moisture and convective parameterizations[22–29].

On the other hand, the convective activity in the tropical atmosphere is organized in the form of planetary-scale structures and exhibits dominant frequencies in the intraseasonal timescale[2,6]. These planetary-scale convective structures originate in the Indian/Western Pacific Oceans and tend to slowly propagate eastward with an irregular speed of $\sim 5m/s$ on average[2]. This phenomenon was labeled as Madden-Julian oscillation (MJO)[30]. The MJO has important socio-economic impacts, being one of the main drivers of tropical monsoons, among other important global effects on weather and climate[31–33]. Understanding and ultimately predicting the initiation, development and propagation of the MJO remain a formidable challenge in tropical meteorology[12]. In particular, the fact that no free equatorial waves having the vertical structure compatible with the atmospheric circulation response to deep convection heating propagate eastward with such a slow phase velocity[34] has originated several theories that attempt to explain the slow propagation of the MJO[35].

It is well established that moisture plays a crucial role in the excitation and propagation of the MJO, with the most accepted MJO theories relying on the coupling between equatorial wave dynamics and the moisture transport equation through convective parameterizations, in what was labeled as *moisture mode theory*[19,20,26,36,37]. Other theories, however, explain the slow eastward propagation of the MJO as a result of the nonlinearity; an example is the *MJO modon theory*[38] in which the MJO is a soliton-like propagating disturbance exhibiting an amplitude-dependent phase speed. Further extensions of the MJO-modon theory have shown that moisture can play the role of either enhancing the stability of the solitary wave solution[39,40] or triggering this eastward propagating disturbance[41,42], although there appears to be more consensus on the latter.

Indeed, Rostami and Zeitlin[41], by adopting a two-layer shallow-water model coupled with the moisture transport equation through a convective adjustment like parameterization, described the

MJO as a hybrid structure disturbance composed of a quasi-equatorial modon coupled with a convectively coupled Kelvin wave. They demonstrated that this hybrid structure MJO-prototype is triggered when the convective heating reaches a threshold anomaly. Moreover, in a recent study, Mayta and Adames-Corraliza[43] analyzed the coupling of propagation structures in the MJO package with moist convection, concluding that the MJO behaves as a moisture mode at the synoptic-scale, but not at the global-scale. Therefore, from the above-mentioned recent findings, the following question is raised: *What controls the MJO propagation at the global-scale?*

The numerical quantification of the MJO phenomenon is often provided by indices that are believed to reflect the MJO activity based on its both circulation and precipitation features[44,45]. In this context, Diaz, Barreiro, and Rubido[46] proposed a data-driven model based on the MJO indices and provided evidence for an amplitude-dependent propagation of the MJO, revealing that nonlinearity plays a significant role in the MJO propagation, especially during El-Niño years.

By performing a decomposition of atmospheric reanalysis field data onto a normal mode function basis (NMF) and a subsequent linear regression between the spectral amplitudes and the MJO indices, Žagar and Franzke[47] identified the primary contributors to MJO variability. They found that the dominant modes of the planetary-scale characteristics of the equatorially trapped component of the MJO are: (i) the first symmetric Rossby mode and (ii) the Kelvin wave mode, both having zonal wavenumber one and the tropospheric baroclinic structure compatible with the atmospheric circulation response to deep convection heating.

In this article, we use the same methodology proposed by Žagar and Franzke[47] in order to select the normal modes that mostly contribute to the MJO variability. By recomposing the physical-space dynamical fields associated with each wave type, we examine the dependence of the propagation properties of the selected waves on their respective amplitudes and the moist convection intensity. In summary, our results indicate that, on a planetary-scale, the equatorial dynamics of the MJO is characterized by a combination of baroclinic Rossby and Kelvin modes, both exhibiting a negative correlation between their amplitudes and propagation frequencies. Furthermore, the propagation speeds of these modes are not found to be significantly correlated with large-scale convective activity. However, a more intricate relationship, involving nonlinear coupling, does exist between planetary-scale convective activity and the propagation speeds of the wave modes.

## III. DATASET

In the normal mode function decomposition procedure utilized here, we used the ERA V reanalysis dataset from the European Centre for Medium-Range Weather Forecasts with $2.5^\circ \times 2.5^\circ$ of horizontal resolution and 137 vertical levels from 1012.05 hPa to 0.01 hPa, with the time period ranging from January 1st 1980 to December 31st 2020.

## IV. METHODS

### A. The atmosphere as a forced-dissipative nonlinear system in the normal mode basis

We may write the equations that govern the large-scale atmospheric dynamics in a vector form as follows:

$$\frac{\partial \mathbf{U}}{\partial t} + \mathcal{L}(\mathbf{U}) = \mathcal{N}(\mathbf{U},\mathbf{U}) + \mathcal{D}(\mathbf{U}) + \mathbf{F}(\mathbf{U},\mathbf{x},t) \tag{1}$$

where $\mathbf{U}(\mathbf{x},t) = (u(\mathbf{x},t), v(\mathbf{x},t), p(\mathbf{x},t))$ is the state vector, with $u$, $v$ and $p$ representing the zonal wind, meridional wind, and pressure fields, respectively; $\mathcal{L}$ is a linear skew-Hermitian operator, $\mathcal{N}$ is a bilinear energy conserving operator containing the advective nonlinearities, $\mathbf{F}(\mathbf{U},\mathbf{x},t)$ is a space and time-dependent forcing term that may represent the parameterization of unresolved physical processes such as thermodynamic/radiative processes, topographic inhomogeneities, among others; $\mathcal{D}$ is a negative definite symmetric operator representing dissipation. Equation (1) may represent different models of the atmospheric flow such as the shallow-water equations, multi-layer shallow-water equations, the Boussinesq equations, and the primitive equations, among others. Here, it will represent the atmospheric primitive equations[48]. By linearizing these equations around a resting basic state, one might solve the inviscid and unforced version of (1) as a linear combination of the eigenfunctions of $\mathcal{L}$:

$$\mathbf{U} = \sum_{\alpha} A_\alpha(t)\varphi_\alpha(\mathbf{x}) \tag{2}$$

where

$$\mathcal{L}(\varphi_\alpha(\mathbf{x})) = i\omega_\alpha \varphi_\alpha(\mathbf{x}) \tag{3}$$

with $\omega_\alpha \in \mathbb{R}$ representing the eigenfrequency associated with the $\alpha$-th eigenvector of $\mathcal{L}$; $A_\alpha(t) \in \mathbb{C}$ represents the spectral amplitude of the $\alpha$-th eigenmode. In such a linear, inviscid, and unforced

version of (1), the spectral amplitude $A_\alpha(t)$ for each $\alpha$ satisfies the following ordinary differential equation:

$$\frac{dA_\alpha}{dt} = i\omega_\alpha A_\alpha, \tag{4}$$

whose solution is given by

$$A_\alpha(t) = A_\alpha(0)e^{i\omega_\alpha t}.$$

Thus, $\omega_\alpha$ represents the rotation rate of the spectral amplitude $A_\alpha$ in the complex plane.

On the other hand, when the nonlinear and forcing terms are restored, the orthogonality and completeness properties of the basis functions $\varphi_\alpha(\mathbf{x})$ allow one to still represent the solution of (1) by the normal mode function series (2). However, the spectral amplitudes $A_\alpha(t)$ in this case satisfy a more complex version of (4) in which the projection of vectors $\mathcal{N}$ and $\mathbf{F}$ onto each eigenvector $\varphi_\alpha(\mathbf{x})$ yields a coupling among different eigenmodes. In this case, denoting the spectral coefficient of the $\alpha$-th eigenmode by $A_\alpha(t) = R_\alpha(t)e^{i\phi_\alpha(t)}$, the corresponding time-frequency $\Omega_\alpha(t) = \dot{\phi}_\alpha(t)$ will, in general, differ from the linear eigenfrequency $\omega_\alpha$. In this case, both nonlinearity and the parameterized physical processes encompassed in the forcing term $\mathbf{F}$ can lead to this time-frequency modification.

For example, the role of nonlinearity in modifying the wave propagation is demonstrated in Raphaldini *et al.*[49] in the context of nonlinear Rossby waves in the barotropic nondivergent model; further examples are found in the context of soliton-like solutions of the atmospheric equations[39,50–52], as well as in Craik[53] for a diversity of physical contexts. Likewise, regarding the parameterized physical processes, there is an extensive range of works demonstrating the role of moist convection in significantly slowing the propagation of large-scale atmospheric waves[6,20,26]. In a recent study, Teruya *et al.*[54] present a comprehensive analysis of wavenumber $\times$ time-frequency spectra of normal-mode decomposed reanalysis data fields, showing that discrepancies between the observed spectra and what is expected from the dry linear theory are more severe than a mere reduction of the phase velocities. Examples were presented in which some eigenmodes exhibit a complete reversion of their propagation speeds for some specific periods, most notably the westward inertio-gravity waves. It was suggested that, at least partially, nonlinearity plays a role in these "anomalously" propagating modes. Therefore, a fundamental question for understanding the physics of convectively coupled equatorial waves is to distinguish, from observations, the nonlinearity and moist convection signatures regarding their roles in modifying

wave propagation.

### B. On the choice of the basis function set

Before describing the projection of the reanalysis data field onto a normal-mode function basis, we shall clarify some common misconceptions regarding the use of the normal mode function approach. In order for a normal-mode function basis to be useful (in the context of atmospheric dynamics), some properties are desirable:

- The basis set should be complete in a suitably defined Hilbert space $\mathcal{H}$. This means that any field $\mathbf{U} = (u, v, p) \in \mathcal{H}$ can be approximated with an arbitrary precision by a linear combination of elements of the normal-mode function basis in $\mathcal{H}$. In other words, for any given $\varepsilon > 0$, there exists an integer $N$ such that:

$$||\mathbf{U} - \sum_{|\alpha| \leq N} A_\alpha \varphi_\alpha|| \leq \varepsilon \tag{5}$$

- The basis set should be time independent. This means that, given any two times $t_1$ and $t_2$, we want the elements of the NMF basis to be the same. This is essential if we want to analyse dynamical features occurring in different times.

- It is desirable that the NMF basis has a relevant physical interpretation. In the case that we use the eigenfunctions of the linear operator $\mathcal{L}$ as the basis function set, as in Eqs. (2)-(3), the interpretation corresponds to the free, dry, linear waves of the corresponding system.

As such, a natural choice for basis set refers to the eigensolutions of the linearized version of the governing equations around a **resting basic state** and with the forcing and dissipation terms being set to zero, as in Eqs. (2)-(3). With that, all the aforementioned desired properties are guaranteed. A common objection to the NMF approach is that the basic state of the atmosphere is no longer at rest. Although certainly, some observed planetary-scale features such as jet streams and Hadley/Walker circulations are long-lived, these planetary-scale features of the atmospheric circulation can themselves be decomposed into the normal mode function basis; this results from the orthogonality and completeness properties of these normal mode functions, which in turn directly follows from the skew-hermitian nature of the linear operator associated with the linearized equations around a resting background state. Indeed, this skew-hermitian property, for example,

is not valid for a linear operator $\mathcal{L}_{\overline{U}}$ resulting from the linearization of the governing equations around a background state characterized by a shear flow, thus the corresponding eigenfunctions does not form a complete basis set in the Hilbert space $\mathcal{H}$. Furthermore, in the framework of Eq. (1), instability processes will be represented by the nonlinear interaction involving the basic state $\overline{U}$ and the wave-modes. This is, in fact, a more complete view of instabilities than the one resulting from linearizing the governing equations around a shear flow that yields the exponential growth of the linear modes, which is only valid for infinitesimal times.

### C. Normal mode decomposition of atmospheric reanalysis data

As mentioned before, the basis function set adopted here to project the global atmospheric field data is given by the eigensolutions of the primitive equations linearized around a resting background state. Adopting the regular spherical coordinate system $(\lambda,\phi)$, with $\lambda$ denoting the longitude and $\phi$ the latitude, and $\sigma = p/p_s$ as the vertical coordinate, where $p$ and $p_s$ denote the pressure and surface pressure fields, respectively, these equations can be written as follows:

$$\frac{\partial u}{\partial t} - 2\Omega v\sin(\phi) = -\frac{g}{a\cos(\phi)}\frac{\partial h}{\partial \lambda}, \tag{6a}$$

$$\frac{\partial v}{\partial t} + 2\Omega u\sin(\phi) = -\frac{g}{a}\frac{\partial h}{\partial \phi}, \tag{6b}$$

$$\frac{\partial}{\partial t}\Big[\frac{\partial}{\partial \sigma}\Big(\frac{g\sigma}{R\Gamma_0}\frac{\partial h}{\partial \sigma}\Big)\Big] - \nabla\cdot\mathbf{V} = 0, \tag{6c}$$

In the equations above, $\mathbf{V} = (u,v)$ is the horizontal velocity field, with $u$ and $v$ denoting its zonal and meridional components, respectively, and $h$ represents the geopotential height; $\Omega$ is the Earth's rotation rate, $a$ the Earth's radius, $g$ the gravity acceleration, $R$ the dry air gas constant, and $\Gamma_0(\sigma)$ refers to the static stability parameter. The eigensolutions of (6) can be written as[55]:

$$\begin{bmatrix} u(\lambda,\phi,\sigma,t) \\ v(\lambda,\phi,\sigma,t) \\ h(\lambda,\phi,\sigma,t) \end{bmatrix} = \mathbf{X}^{(\alpha)}_{m,k,n}(\phi)\exp[ik\lambda - i\omega^{(\alpha)}_{m,k,n}t]G_m(\sigma) \tag{7}$$

In (7), each eigenmode is labeled by the vertical mode index m, the zonal wavenumber k, the meridional quantum index n and the mode type denoted by $\alpha$; the vertical structure functions

$G_m(\sigma)$ satisfy a rigid lid boundary condition Sturm-Liouville problem, while the meridional structure vector functions $\mathbf{X}^{(\alpha)}_{m,k,n}(\phi)$ and the eigenfrequencies $\omega^{(\alpha)}_{m,k,n}$ satisfy the eigenvalue problem (3) with the operator $\mathcal{L}$ being given by

$$\mathcal{L} = \begin{bmatrix} 0 & -2\Omega\sin(\phi) & \frac{ikg}{a\cos(\phi)} \\ 2\Omega\sin(\phi) & 0 & \frac{g}{a}\frac{d}{d\phi} \\ \frac{ikH_m}{a\cos(\phi)} & \frac{H_m}{a}\frac{d}{d\phi}(cos\phi) & 0 \end{bmatrix} \tag{8}$$

where $H_m$ is the separation constant, also known as equivalent height[56]. The eigenvalue problem described above was solved by Longuet-Higgins[57], Kasahara[58] and Kasahara[59], and its eigensolutions refer to the so-called westward/eastward propagating inertio-gravity waves, the Rossby-Haurwitz waves, the mixed Rossby-gravity waves and the Kelvin modes.

The orthogonality and completeness properties of the eigensolutions described above allow one to represent the observed horizontal wind and geopotential height fields in terms of the following series:

$$\mathbf{X}(\lambda,\phi,\sigma,t) = \begin{bmatrix} u(\lambda,\phi,\sigma,t) \\ v(\lambda,\phi,\sigma,t) \\ h(\lambda,\phi,\sigma,t) \end{bmatrix} = \sum_{m=0}^{\infty}\sum_{k=-\infty}^{\infty}\sum_{n=0}^{\infty}\sum_{\alpha}\chi^{(\alpha)}_{m,k,n}(t)\mathbf{X}^{(\alpha)}_{m,k,n}(\phi)e^{ik\lambda}G_m(\sigma) \tag{9}$$

Consequently, given the global data of the horizontal wind and geopotential height fields $\mathbf{X}(\lambda,\phi,\sigma,t) = (u,v,h)^T$, the expansion coefficients $\chi^{(\alpha)}_{m,k,n}(t)$ are obtained by the projection of the observed field data onto each element of the basis function set:

$$\chi^{(\alpha)}_{m,k,n}(t) = \int_0^1\int_0^{2\pi}\int_{-\pi/2}^{\pi/2}\langle\mathbf{X}(\lambda,\phi,\sigma,t),\mathbf{X}^{(\alpha)}_{m,k,n}(\phi)\rangle\cos(\phi)e^{-ik\lambda}G_m(\sigma)d\phi d\lambda d\sigma. \tag{10}$$

where $\langle .,. \rangle$ denotes the Euclidean scalar product in $\mathbb{R}^3$.

The procedure described above was first proposed by Kasahara and Puri[55]; here we have used a recent implementation of this procedure provided by the open-source MODES software described by Žagar *et al.*[60]. The normal mode approach has been used in the study of several low-frequency atmospheric phenomena[60–62]; the detailed procedure for selecting certain normal modes from climate indices will be described in the next section.

### D. MJO-related mode selection

The quantification of the Madden-Julian Oscillation (MJO) activity is usually performed by using one of its indices that have been proposed to describe different features associated with the MJO[16,45,63]. These indices are calculated by using the two first empirical orthogonal functions (EOFs) of circulation and/or outgoing-long-wave radiation (OLR) fields. Here, we use the OLR-based MJO index (OMI)[45] and follow the approach of Žagar and Franzke[47] in which the time-series of the normal mode spectral coefficients $\chi^{(\alpha)}_{m,k,n}(t)$ are regressed against the MJO index $Y(t)$ (representing the first OMI EOF; results for the second EOF are very similar and will be omitted here):

$$\mathcal{R}^{(\alpha)}_{m,k,n} = \frac{1}{N-1}\sum_{t=1}^{N}\frac{(\chi^{(\alpha)}_{m,k,n}(t) - \overline{\chi^{(\alpha)}_{m,k,n}})(Y(t)-\overline{Y})}{Var(Y(t))} \tag{11}$$

where the operator "$\overline{()}$" denotes the time averaging referred to the whole analysis period (e.g., from January 1st 1980 to December 31st 2020), and $\mathcal{R}^{(\alpha)}_{m,k,n}$ represents the regression coefficient. Given the regression coefficients $\mathcal{R}^{(\alpha)}_{m,k,n}$, the MJO variance due to a particular mode $(m,k,n,\alpha)$ can be written as:

$$V^{(\alpha)}_{m,k,n,} = gH_m\mathcal{R}^{(\alpha)}_{m,k,n}(\mathcal{R}^{(\alpha)}_{m,k,n})^* \tag{12}$$

where the superscript "$*$" indicates the complex conjugate. The computed variance spectrum is displayed in Fig. 1 for each mode type (rotational modes and the eastward/westward propagating inertio-gravity modes) as a function of the zonal wavenumber k, the meridional index n and the vertical mode index m. Since the eastward propagating inertio-gravity modes having the first meridional index n = 0 refer to the Kelvin waves[58], Fig. 1a shows that the MJO is dominated by the k = 1 Kelvin and first symmetric (n = 1) Rossby modes. In addition, from Fig. 1c one notices that the peak of the Kelvin mode component of the MJO variance spectrum is on vertical modes m = 8-9. As illustrated in Fig. 2, the vertical structure functions referred to these modes are characterized by a baroclinic structure in the troposphere that exhibits a phase inversion between its lower and upper layers. This baroclinic structure is compatible with the vertical profile of the tropical circulation response to deep convection heating[14]. On the other hand, regarding the k = 1 Rossby waves with n = 1 that mostly contribute to the MJO variability, these modes are dominated by the lowest vertical modes (m = 1 and 2), with a second peak coinciding with the Kelvin mode one (m = 8-9). As can be noticed from Fig. 2, the lowest vertical modes m = 1 and 2 are

characterized by a barotropic structure in the troposphere, and the meridional structure functions of the eigenmodes having these vertical mode indices are no longer trapped within the tropics, exhibiting in contrast a large amplitude in middle and high latitudes[58]. In fact, the Rossby waves exhibiting a barotropic structure throughout the troposphere are known to be responsible for the tropics-extratropics teleconnections[64,65]. Therefore, these barotropic Rossby modes that mostly contribute to the MJO variability might be associated with the tropics-extratropics teleconnections associated with the MJO[66], whereas the Kelvin and the first symmetric Rossby modes having vertical modes $7 < m < 10$ and zonal wavenumber k = 1 represent the dominant modes for the tropical component of the MJO variability.

The way in which tropical heat sources such as those associated with the MJO can give rise to a barotropic Rossby wave response has been a topic of considerable research effort. It has been suggested that this excitation is due to the different mechanisms that couple the baroclinic structure equatorially trapped wave modes that are directly forced by the tropical heat sources and the barotropic Rossby modes; these coupling mechanisms include the vertical shear of the background flow[67–70], the differential damping between the lower and upper troposphere[67] and the nonlinearity[9–11]. Moreover, this relationship between the MJO convective activity and the barotropic Rossby modes verified in Fig. 1 is also in agreement with the observational analysis of Wang, Yano, and Lin [71], who found a strong correlation between the global vorticity patterns related to barotropic Rossby wave trains and the tropical pattern of the outgoing longwave radiation (OLR) related to the MJO. Furthermore, the tropical vorticity pattern related to the MJO variability found by Wang, Yano, and Lin [71] was characterized by a symmetric about the equator dipole vortex structure slowly propagating eastward, which is consistent with the MJO modon theory[38–40]. Since the linear Rossby wave dispersion relation gives a westward phase propagation, the eastward propagation referred to the Rossby modon reflects a strongly nonlinear effect. In fact, in the modon-based scenario, the eastward MJO propagation is associated with the nonlinearity, with moist convection playing the role of triggering the MJO structure. As will be shown later, the results presented in Sections V and VI are consistent with this idea.

Indeed, Fig. 3 shows the time-series of the amplitudes $|\chi^{(\alpha)}_{m,k,n}|$ associated with the equatorially trapped modes that mostly contribute to the MJO variability. From Fig. 3 one notices that the amplitudes of these MJO-related normal modes undergo significant modulations in time. On the other hand, as in the linear and unforced/inviscid context the spectral amplitudes $|\chi^{(\alpha)}_{m,k,n}|$ would remain constant in time according to Eq. (4), these amplitude modulations observed in Fig. 3

result from the effects of either the advective nonlinearity or the parametric forcings associated with the parameterization of thermodynamic processes related to moist convection, as will be further discussed in the next sections.

It is also possible to notice from Fig. 3 that the amplitudes of the Kelvin modes undergo a higher variability than the Rossby mode amplitudes. This higher variability of the Kelvin mode amplitudes might be attributed to the broader range of nonlinear interactions involving this wave type. Indeed, as will be discussed later, the Kelvin modes may encompass the multi-scale interactions involving synoptic-scale and planetary-scale convective disturbances that excite the planetary-scale structure associated with the MJO.

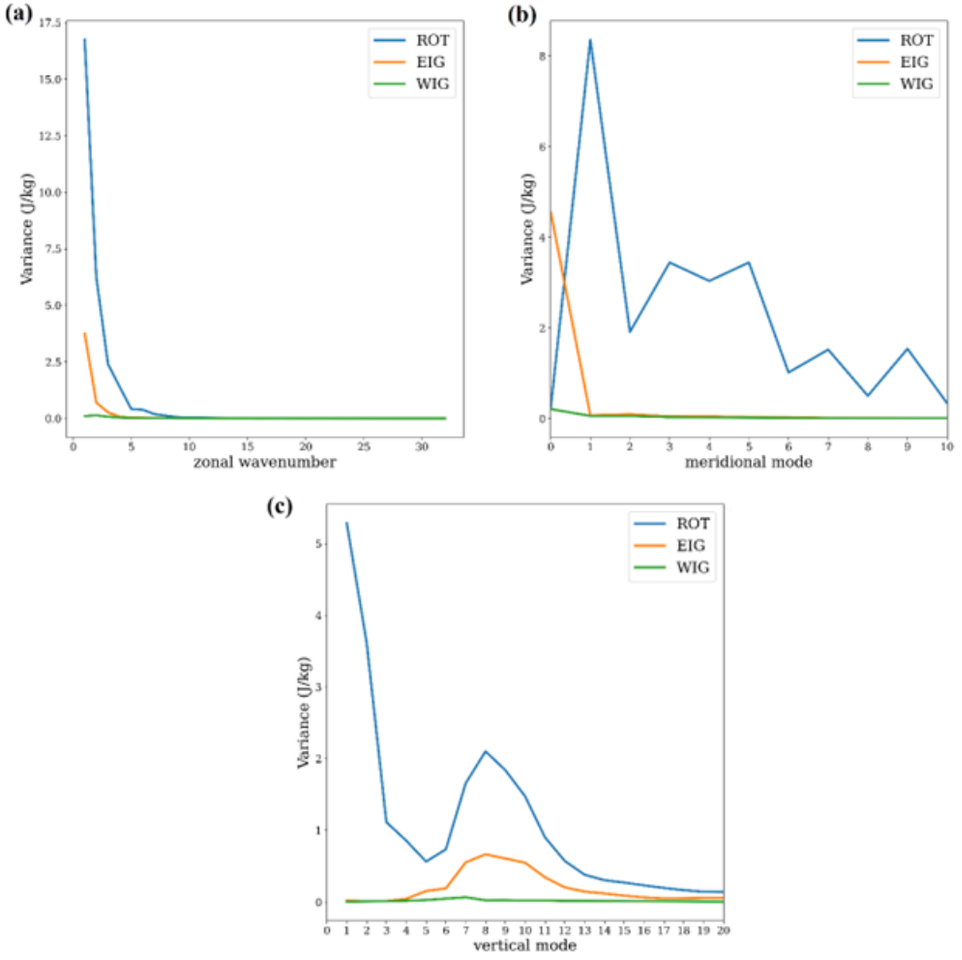


FIG. 1. Variance spectrum associated with the regression coefficients of the normal mode amplitudes against the first EOF of the OMI index of the MJO, as a function of the zonal wavenumber k (a), the meridional index n (b) and the vertical mode index m (c).

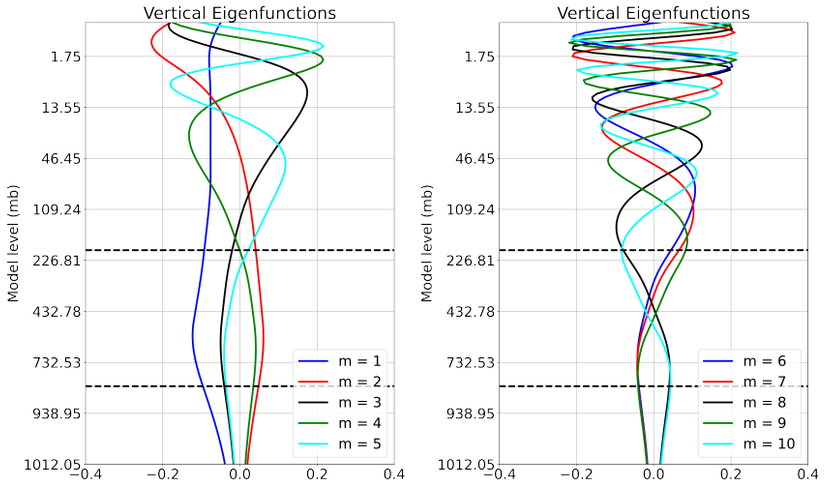


FIG. 2. Vertical structure functions referred to the vertical mode indexes $1 \leq m \leq 10$. The dashed lines indicate the reference pressure levels of the lower (850hPa) and upper (200hPa) troposphere.

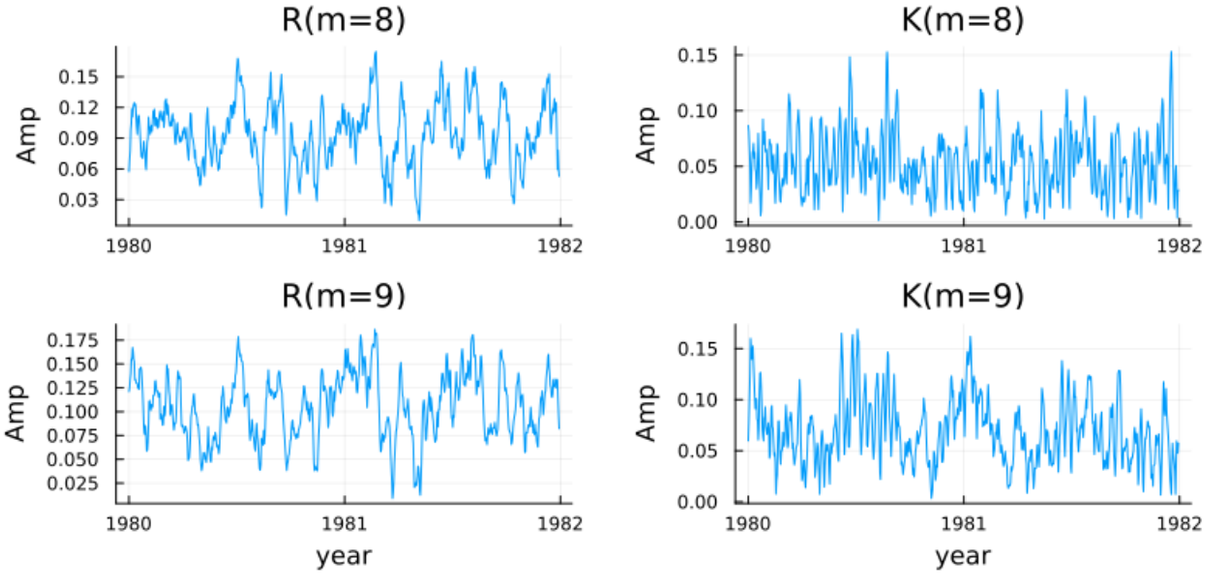


FIG. 3. Time series of the amplitudes $|\chi^{(\alpha)}_{m,k,n}(t)|$ of the Rossby (left panels) and Kelvin (right panels) modes with zonal wavenumber k = 1 and vertical mode indices m =7, 8 and 9; the Rossby modes refer to the first symmetric ones (meridional quantum index n = 1). The vertical mode indices are indicated in each panel.

### E. Sindy Method

To evaluate the functional form of the moisture influence on the amplitudes of the MJO-related normal modes, we shall apply the SINDy (*Sparse Identification of Nonlinear Dynamics*) technique[72]. Suppose that we have observed a vector-valued time-series $\mathbf{X}(t) \in \mathbb{R}^n$, the problem is to infer from the data the differential equation that governs the evolution of $\mathbf{X}(t)$:

$$\frac{d\mathbf{X}(t)}{dt} = \mathbf{F}(\mathbf{X}(t)) \tag{13}$$

where $\mathbf{F} : \mathbb{R}^n \to \mathbb{R}^n$ is a smooth vector field. Thus, the problem consists of discovering the vector operator $\mathbf{F}$. As such, the question is too general since $\mathbf{F}$ lies in an infinite dimensional space. If, however, $\mathbf{F}$ is analytic, it can be approximated with arbitrary precision by polynomial functions:

$$\mathbf{F}(\mathbf{X}(t)) = \sum_{\gamma} a_\gamma x_1^{\gamma_1} x_2^{\gamma_2} ... x_n^{\gamma_n} \tag{14}$$

where $\gamma = (\gamma_1, \gamma_2, ..., \gamma_n)$ is a *multi-index*, with $\gamma_j \in \mathbb{N}$ for all $j = 1, 2, ..., n$. For a given $\gamma$, the order of the corresponding monomial is given by $|\gamma| = \gamma_1 + \gamma_2 + ... + \gamma_n$. In practice, we truncate the expansion (14) to a fixed order ($|\gamma| \leq K$), and search for an approximation of $\mathbf{F}$ in a monomial basis $\mathcal{B} = \{\mathbf{x}^\gamma\}_{|\gamma| \leq K}$:

$$\overline{\mathbf{F}} = \sum_{|\gamma| \leq K} a_\gamma x_1^{\gamma_1} x_2^{\gamma_2} ... x_n^{\gamma_n} \tag{15}$$

Since we can estimate the time derivative of $\mathbf{X}$ from the available time-series data, denoted by $\mathbf{X}'$, the SINDy algorithm seeks the set of amplitudes $a_\gamma, |\gamma| \leq K$, that minimizes the $L^2$ distance between $\mathbf{X}'$ and $\overline{\mathbf{F}}(\mathbf{a}; \mathbf{X})$. Thus, the optimization problem consists of finding

$$\mathbf{a}^* = argmin_a ||\mathbf{X}' - \overline{\mathbf{F}}(\mathbf{a}; \mathbf{X})||_2 + \lambda ||\mathbf{a}||_1 \tag{16}$$

where the last term $\lambda ||\mathbf{a}||_1$ is a regularizing term that is included to promote *sparsity* in the optimization problem[72]. The SINDy method has been recently used to analyze the dynamics of the MJO from its indices[46].

## V. AMPLITUDE DEPENDENCE ON TCWV FOR SELECTED NORMAL MODES

As previously mentioned, moisture plays a central role in most of the MJO theories[35]. For instance, in the moisture mode theories of the MJO[20,26], the background climatological moisture field yields unstable modes that couple the large-scale dynamics and moist convection. According to Mayta and Adames Corraliza [73], these moisture modes occur in regions where the moisture horizontal gradient is high, and their instability is related to a diffusive poleward moisture flux. In addition, in the MJO skeleton theory, the low-level moisture field destabilizes synoptic-scale waves, which in turn excite the global-scale Kelvin-Rossby structure of the MJO by the upscale momentum and heat fluxes[24,74]. Likewise, recent versions of the modon theory argue that the moisture acts to trigger the solition-like disturbance that composes the MJO[41,42]. Therefore, in this section we investigate how the moisture field interacts with the normal modes that mostly contribute to the MJO variability within the tropics. As shown in Section IV D, these normal modes refer to the Kelvin and the first symmetric (n = 1) Rossby modes, both having zonal wavenumber-1 and the baroclinic structure in the troposphere compatible with the tropical circulation response to deep convection heating[14] (i.e., vertical mode indexes m = 8-9).

To describe the relationship between the amplitudes of these MJO-related normal modes and the moisture field, we use the *total column water vapor (TCWV)* time-series. The TCWV time-series is computed in the equatorial belt from $10°S$ to $10°N$. In the longitudinal direction, we integrate the TCWV field in the *Indo-Pacific warm pool* region, which is known to be crucial for the MJO dynamics[75,76]. The *Indo-Pacific warm pool* region is subdivided into three sub-regions, namely: (i) the *Indian Ocean (IO)* sector, from 60°E to 100°E, (ii) the *Maritime Continent (MC)* sector, from 100°E to 140°E, and (iii) the *Western Pacific (WP)* region, from 140°E to 180°. Thus, we have three times-series that are representative of the TCWV signals at three different regions of the equatorial belt (IO, MC and WP), and we have computed their correlations with the amplitudes $|\chi^{(\alpha)}_{m,k,n}(t)|$ of the aforementioned planetary-scale Kelvin and Rossby modes. For comparison, these correlations have been computed for active and inactive MJO days. We have selected the active days as the ones exhibiting $|OMI| > 1.5$. While this definition is somewhat arbitrary, we have tested with various thresholds to assess the sensitivity of the results. However, the chosen threshold did not significantly alter the results. In contrast, to make a clearer distinction with the active days, the inactive ones have been selected by considering $|OMI| < 0.8$.

The results referred to the Indian Ocean sector are displayed in Figure 4, which shows the

scatter-plots of the mode amplitudes against the TCWV in the IO region (denoted simply by *IO*). The correlations and p-values are indicated at the top of each panel. In this region, which is known to be the region of the globe where the convective activity related to the MJO initiates, the correlations between the normal-mode amplitudes and the TCWV displayed in Fig. 4 are all consistently negative, especially for active MJO days.

This result appears to be consistent with the results of Mayta and Adames-Corraliza[43], who showed that in the IO sector the MJO behaves as a moisture mode and is characterized by a synoptic-scale rather than the planetary-scale associated with the wave modes analyzed here. In fact, according to the skeleton theoretical model of the MJO[24,25], the synoptic-scale convective disturbances are primarily excited, transferring energy to the planetary-scale convective disturbances afterwards; these planetary-scale convective disturbances (defined by the authors as the convective or wave activity variable), in turn, excite the planetary-scale Kelvin and Rossby modes by a heat forcing mechanism. This upscale energy transfer from synoptic-scale to planetary-scale disturbances in the MJO skeleton model is described in detail by the multi-scale model of the MJO dynamics presented by Biello and Majda[74]. In this scenario, the results displayed in Fig. 4 suggest that in the initial phase of the convection organization associated with the MJO, the planetary-scale waves lose their energy to the synoptic-scale disturbances related to the convective activity of the MJO in the IO sector. Indeed, Roundy[77] highlighted the modulation of synoptic-scale convectively coupled Kelvin waves by the planetary-scale circulation related to the MJO in the Indian Ocean. Furthermore, observation evidence for the interaction between synoptic-scale westward inertio-gravity modes and Kelvin waves was presented by Teruya *et al.*[54].

Figure 5 displays the results referred to the *Maritime Continent* region. Unlike the IO case displayed in Fig. 4, the correlations between the normal mode amplitudes and the TCWV are either slightly positive or statistically zero for the Maritime Continent (MC) sector. For the Kelvin modes, the correlations are statistically zero for inactive MJO and statistically positive for active MJO periods. In contrast, for the Rossby modes, the correlations are all consistently positive and do not exhibit significant differences between active and inactive MJO cases, being even slightly smaller for active days for the m = 8 vertical mode. For the *Western Pacific* region, the results are presented in Figure 6 and show that the correlations are statistically zero for inactive and consistently positive for active MJO periods.

The interpretation of the results displayed in Figs. 5 and 6 for the *Maritime Continent* and *Western Pacific* regions can be made in the context of the MJO skeleton theory[24,25]. In this context,

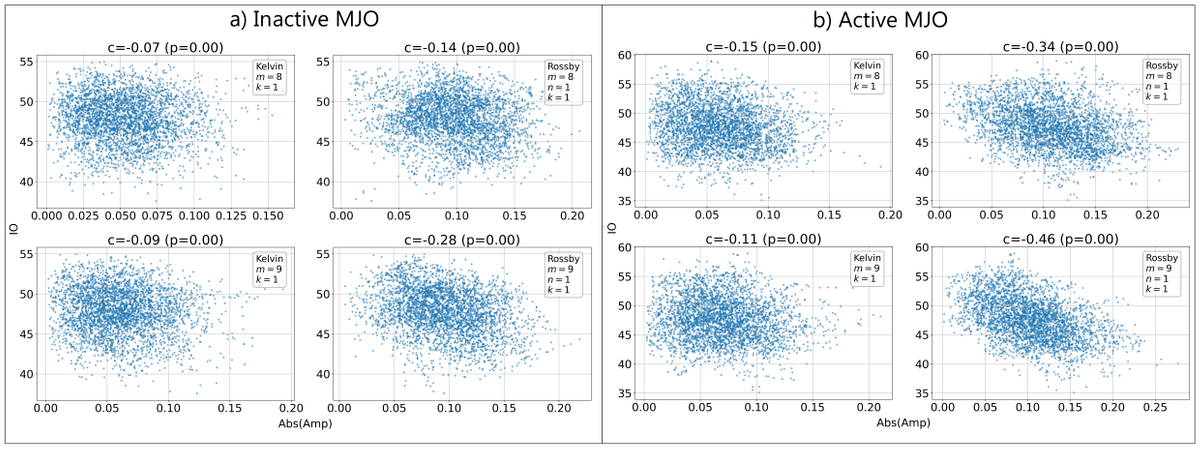


FIG. 4. Scatter diagrams between the total column water vapor (TCWV) over the equatorial Indian Ocean (IO; 10°$S$ - 10°$N$ and 60°E - 100°E) sector and the amplitudes $|\chi^{(\alpha)}_{m,k,n}|$ of the Kelvin and Rossby modes that mostly contribute to the tropical variability of the MJO, for active (a) and inactive (b) periods of the MJO convective activity. The zonal wavenumbers $k$, meridional indices $n$, vertical mode indices $m$ and the wave types (Kelvin or Rossby) are displayed in each panel. The respective linear correlations and p-values are displayed at the top of each panel.

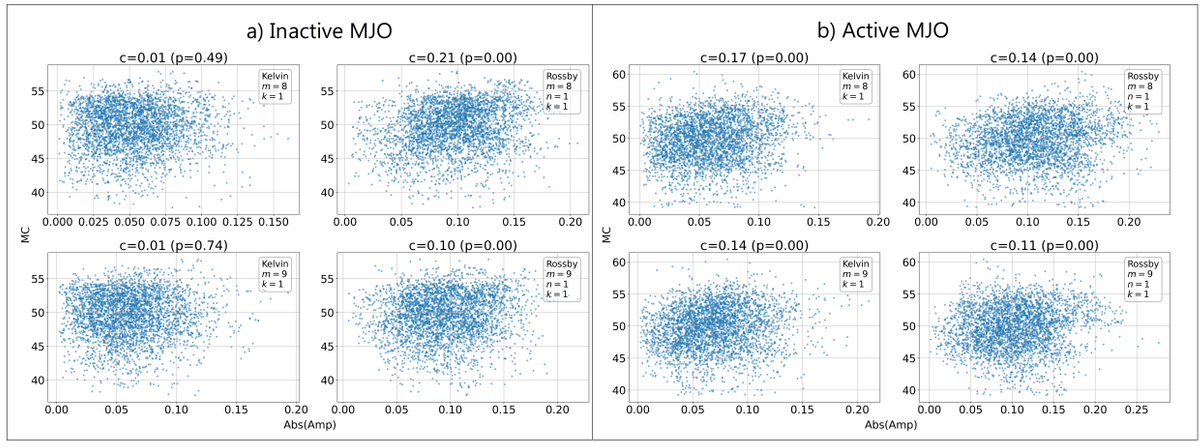


FIG. 5. Similar to Fig. 4, but for the TCWV over the equatorial maritime continent (MC; 10°S - 10°N and 100°E - 140°E) sector.

the results suggest that the upscale energy transfer from synoptic-scale toward planetary-scale convective disturbances that is believed to excite the Kelvin-Rossby planetary-scale structure of the MJO occurs for the Kelvin modes, and then these modes subsequently transfer their energy to the

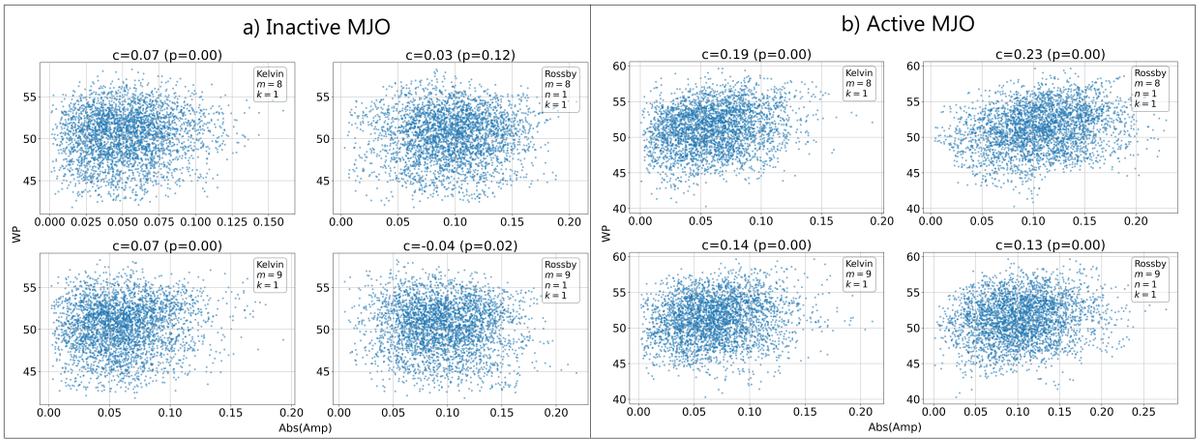


FIG. 6. Similar to Fig. 4, but for the TCWV at the equatorial Western Pacific (WP; 10°S - 10°N and 140°E - 180°) sector.

Rossby modes. This possible conjecture is in agreement with the causality analysis documented in Raphaldini *et al.* [78] for these MJO related waves, in which the authors showed that the Kelvin mode is initially driven by the MJO convection and subsequently excites the Rossby wave component of the MJO. This possible conjecture is also corroborated by the results obtained by applying the SINDy method, as will be described next.

To further investigate the relationships between the amplitudes of the selected MJO-related normal modes and the moisture field, we use the SINDy technique[72] to adjust a system of ordinary differential equations representing the behavior of the normal mode amplitudes and the moisture variable. In order to keep the system easily comprehensible, we reduce the number of variables. Given that the relationships between the normal mode amplitudes and the TCWV are similar for the *Maritime Continent* and *Western Pacific* regions for active MJO periods, we have grouped them into a single variable labeled as $M$, which refers to the average of the TCWV at these two sectors. Similarly, the Rossby and Kelvin wave amplitudes displayed in Figures 4-6 are combined into a single amplitude variable for each wave-type by integrating throughout the vertical mode range $8 \leq m \leq 9$, namely:

$$R(t) = \sqrt{\sum_{m=8}^{9} \left( g H_m |R_{m,1,1}(t)|^2 \right)} \tag{17}$$

$$K(t) = \sqrt{\sum_{m=8}^{9} \left( g H_m |K_{m,1}(t)|^2 \right)} \tag{18}$$

Thus, $R$ and $K$ represent the combined amplitudes for the Rossby and Kelvin modes, respectively, that mostly contribute to the tropical variability of the MJO. Consequently, we have three variables, one representing TCWV (variable M), averaged over the equatorial belt ($10^\circ S - 10^\circ N$) referred to the longitude sector from 100°E to 180°, and the other two representing the Rossby and Kelvin wave amplitudes ($R$ and $K$, respectively). In order to normalize these three time-series we have computed their respective Z-scores:

$$\tilde{X}(t) = \frac{X(t) - \overline{X}}{\sigma_X} \tag{19}$$

where the variable $X$ in the equation above can denote $M$, $R$ or $K$, with mean $\overline{X}$ and standard deviation $\sigma_X$. Thus, given the Z-scored variables $\tilde{M}$, $\tilde{R}$ and $\tilde{K}$, we have used the PySINDy package[79], available at https://pysindy.readthedocs.io/en/latest/, with its *ensemble* functionality that computes an average model from a model ensemble by under-sampling the datasets. We have computed 1000 models, each of them randomly leaving 40% of the data out of the procedure. The resulting equations governing the time evolution of these variables are given by:

$$\frac{dM}{dt} = -0.031R - 0.015K - 0.011MR + 0.003MK + 0.004R^2 + 0.002K^2 \tag{20a}$$

$$\frac{dR}{dt} = 0.033M - 0.022R + 0.054K + 0.005M^2 - 0.002MR + 0.003MK - 0.002R^2 + 0.013RK - 0.011K^2 \tag{20b}$$

$$\frac{dK}{dt} = 0.024M - 0.052R + 0.023K - 0.010MR + 0.006MK - 0.007R^2 + 0.002RK - 0.001K^2 \tag{20c}$$

where in the equations above we have omitted the "˜" to denote the Z-scored variables for simplicity. The distribution (histogram) of the coefficients inferred from the analysis is displayed

in Fig. 1 of the *Supplementary Material*. Here we present only the coefficients that were found to be statistically different from zero. The magnitudes of the coefficients in the governing equations for the Rossby and Kelvin wave amplitudes suggest that Rossby and Kelvin wave amplitudes are influenced by the magnitude of the TCWV variable, with a strong positive linear dependence of $\frac{dR}{dt}$ and $\frac{dK}{dt}$ on $M$. Another interesting feature is that the moisture can promote an energy exchange between Rossby and Kelvin waves; this can be noticed from the term proportional to $M \cdot R$ in the equation for the Kelvin-wave amplitude and the term proportional to $M \cdot K$ in the equation for the Rossby wave amplitude. Basically, these terms mean that energy is removed from the Kelvin modes and transferred to the Rossby modes via the moisture field. Furthermore, the term proportional to $\mathrm{M} \cdot K$ in the equation of the Kelvin wave amplitude indicates that an enhanced moisture field can promote a linear instability on the global-scale Kelvin modes.

These results are consistent with the causality analysis between the same global-scale Kelvin and Rossby modes performed in Raphaldini *et al.*[78], which suggests that the Kelvin waves are the first ones to be excited and subsequently transfer energy to the Rossby waves, as previously mentioned. In addition, the cross-linear terms that promote the interaction between Rossby and Kelvin waves through moisture resemble the linear wave interaction mechanism involving two equatorial wave modes through the background moisture filed in the context of a deep convection parameterization[80]. Raupp and Silva Dias[80] used the equatorial $\beta$-plane primitive equations in the presence of a heat source that is parameterized according to the so-called wave-CISK hypothesis[81,82]; they showed that an equatorial inertio-gravity wave mode may interact with (and excite) an equatorial Rossby wave mode through resonance with the diurnal cycle of the background moisture field.

Similarly, the terms $0.054K$ and $-0.052R$ in the equations for the Rossby and Kelvin modes, respectively, work in the same way as the corresponding terms proportional to $MK$ and $MR$ in their respective equations, promoting an interaction between Kelvin and Rossby wave modes, making the energy to be extracted from the former and transferred to the latter. It is possible that the terms $0.054K$ and $-0.052R$ be associated with the background moisture field, or the time independent part of the TCWV field, whereas the terms proportional to $MK$ in the Rossby wave equation and $MR$ in the Kelvin wave equation can be associated with the anomaly or the time-dependent part of the moisture field, with this anomaly being essentially due to the seasonal cycle. Indeed, in the context of the linear wave interaction mechanism involving Rossby and inertio-gravity modes proposed by Raupp and Silva Dias[80], it was shown that the dynamics of this interaction is strongly

dependent on the latitude of the forcing. Apart from the background moisture field, the waves can also interact through other spatial inhomoganeities such as topographic variations[83,84].

Although the application of the SINDy technique to atmospheric normal modes associated with the MJO allows one to compare it with theoretical/mechanistic models, such as the theoretical models of wave interactions mentioned above, it also comes with some limitations. First, these normal modes do not constitute an isolated system. Rather, they are connected with other normal modes that have not been considered here, which in turn may influence the normal modes analyzed here through nonlinear interactions. Second, the MJO itself depends on other factors such as the El Niño Southern Oscillation[46], the quasi-biennial oscillation[62], the seasonality[85] and the climate change[75]. Each of these dependencies are beyond the scope of the present study and are worth of investigation in the future. The statistics of the SINDy analysis was performed via resampling techniques (i.e. emsamble SINDy) indicating some robustness in the computation of the SINDy terms, although the aforementioned external factors are no longer random.

## VI. FREQUENCY-AMPLITUDE DEPENDENCE OF THE SELECTED NORMAL MODES

A central question regarding the dynamics of the Madden-Julian Oscillation refers to the mechanisms that drive its slow eastward propagation[2,35]. In this context, moisture does play a central role in most of the theoretical attempts to address this issue, including the wave-CISK formulation[86,87], the boundary-layer frictional convective convergence mechanism[88], as well as the recent attempts that consider the feedback between the wave dynamics and the moisture transport equation such as the multi-cloud convective parameterization models[27–29] and the moisture-mode theories[20,76,89]. Nevertheless, other theories explain the MJO as a soliton-like disturbance with an amplitude dependent propagation[39,52], thus pointing out the nonlinearity as the key mechanism to slow down the propagation speed of the MJO disturbance. Recently, Mayta and Adames-Corraliza[43] analyzed the propagation of oscillations within the MJO package, concluding that the MJO appears a moisture mode at the synoptic-scale (zonal wave-numbers $3 \leq k \leq 6$), but probably not on the global-scale. Therefore, if there is not a strong coupling between the wave dynamics and moisture at the global-scale, what does it determine the propagation at this scale?

To address this question, here we examine the dynamics of the instantaneous nonlinear frequency of the selected MJO-related normal modes. Expressing the spectral coefficients in the

polar form,

$$\chi^{(\alpha)}_{m,k,n}(t) = |\chi^{(\alpha)}_{m,k,n}(t)|e^{i\phi^{(\alpha)}_{m,k,n}(t)},$$

the instantaneous nonlinear frequency of a given mode $(m,k,n,\alpha)$ is defined by

$$\tilde{\omega}^{(\alpha)}_{m,k,n}(t) = \frac{d\phi^{(\alpha)}_{m,k,n}(t)}{dt} \tag{21}$$

where $\phi^{(\alpha)}_{m,k,n}(t) = \arg(\chi^{(\alpha)}_{m,k,n}(t))$ denotes the mode's phase. As discussed in Section IV A, the instantaneous frequency $\tilde{\omega}^{(\alpha)}_{m,k,n}(t)$ can significantly differ from the linear eigenfrequency $\omega^{(\alpha)}_{m,k,n}$ due to the effects of both nonlinearity and the parameterized forcing mechanisms, in particular the physical processes associated with moisture.

Fig. 7 presents the histograms referred to the daily values of the instantaneous propagation speeds, $\tilde{\omega}^{(\alpha)}_{m,k,n}(t)/k$, of the selected Rossby and Kelvin modes. These histograms are presented separately for active and inactive MJO days. For comparison, we plot the free linear propagation speed of the corresponding normal mode represented by vertical red lines, as well as the reference speed of *5 m/s* (vertical dashed lines) that corresponds to the typically observed propagation speed of the MJO. First, the histograms for the propagation speeds of the Kelvin modes present a bimodal distribution, in which the dominant peak corresponds to a stationary/slow propagation regime, with the *typically observed* MJO speed of $5ms^{-1}$ being comprised by this peak. On the other hand, the secondary peak corresponds to the propagation speed of the free linear Kelvin waves. The Rossby waves also present histograms with a dominant peak that is significantly slower than the free linear waves. However, unlike the Kelvin waves, the Rossby modes exhibit histograms with an uni-modal character. In both cases, there is a clear tendency for a stationary/slowly propagating behavior in the active MJO cases.

In the theoretical point of view, the faster/dry propagation regime can be understood in terms of the linear adjustment problem to a localized heat source[14,90] in a dry environment, where in the long wave limit the response is characterized by a linear combination of westward propagating Rossby and eastward propagating Kelvin waves. On the other hand, the stationary/slowly propagating regime for these planetary-scale wave modes can be understood in terms of the nonlinear geostrophic adjustment problem in a moist atmosphere[91]. Indeed, Rostami and Zeitlin[91] adopted a nonlinear shallow-water model coupled with the moisture transport equation through a moist convective adjustment like parameterization and showed that, when the heating reaches a threshold anomaly, the above-mentioned Matsuno-Gill's solution is replaced by slowly eastward

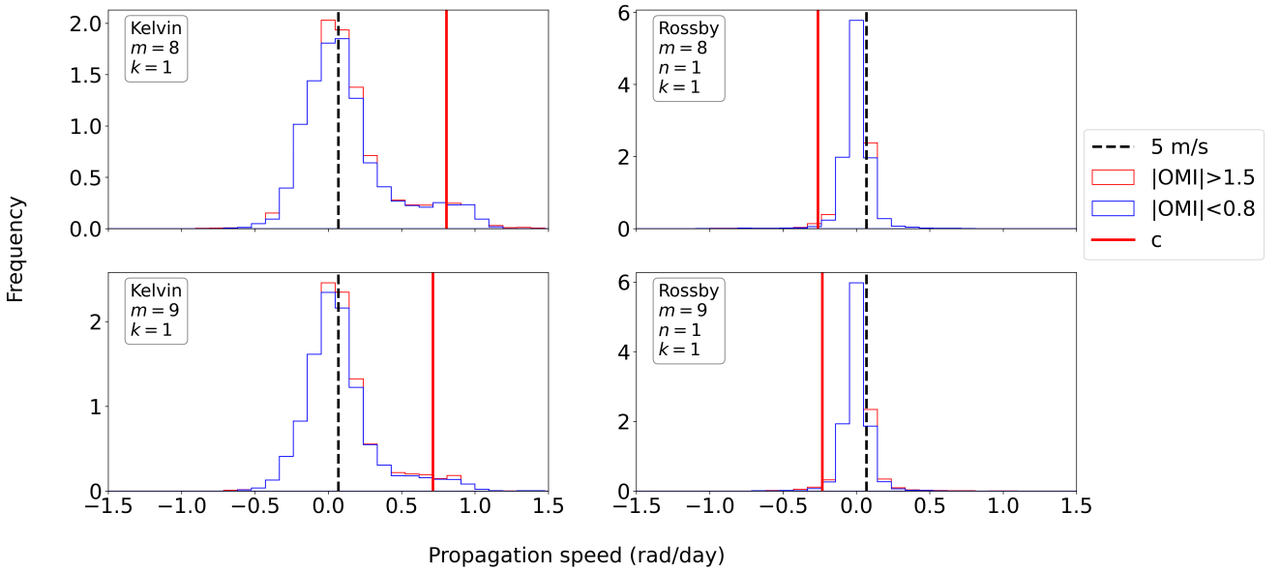


FIG. 7. The histograms represent the daily values of the propagation speed of Kelvin (left panels) and Rossby (right panels) modes for both active days ($|OMI| > 1.5$) and inactive days ($|OMI| < 0.8$) of the MJO. The zonal wavenumber $k$, the vertical mode index $m$, and the meridional quantum number $n$ associated with each eigenmode are displayed at each panel, as well as the corresponding phase velocity predicted by the dry linear theory (red line) and the reference value of $5ms^{-1}$ (dashed line) associated with the typically observed propagation speed of the MJO.

propagating vortical structures that are reminiscent of the equatorial Rossby modons. Another possible conjecture refers to the MJO skeleton theory[24,25], in which the coupling of the ultra-long Rossby and Kelvin wave packets with the moist convective activity and the moisture field yields a slowly eastward propagating structure with an approximately zero group velocity.

Therefore, it is important to infer from our dataset the mechanisms that differ the stationary/slowly propagating regime from the faster/freely propagating one. To address this point, we first investigate the dependency of the instantaneous frequency of the MJO-related normal modes on the TCWV variables restricted to the *Indian Ocean (IO)*, *Maritime Continent (MC)* and *Western Pacific (WP)* sectors. Now, we restrict our analysis to active MJO days ($|OMI| > 1.5$). The scatter plots of the normal mode instantaneous frequencies against the IO-TCWV are displayed in Figure 8. These plots show a weak correlation between the instantaneous frequencies and the IO-TCWV for the Kelvin waves, while a slightly positive correlation is found for the Rossby modes.

For comparison, the eigenfrequencies of these modes predicted by the dry linear theory (Eq. 6) are plotted in each panel as a red line. As in the case of the normal mode amplitude analysis, the dependencies of the normal mode phases on the MC and WP TCWV are similar for active MJO days and are shown in Figures 9 and 10, respectively. For these two regions, the Kelvin waves exhibit a slightly negative, yet significant, correlation between their instantaneous frequency and the TCWV, with correlation coefficients $-0.12 < c < -0.09$. On the other hand, the correlation between the instantaneous frequency and the MC/WP TCWV is even weaker, and in some cases not statistically significant, for the Rossby modes.

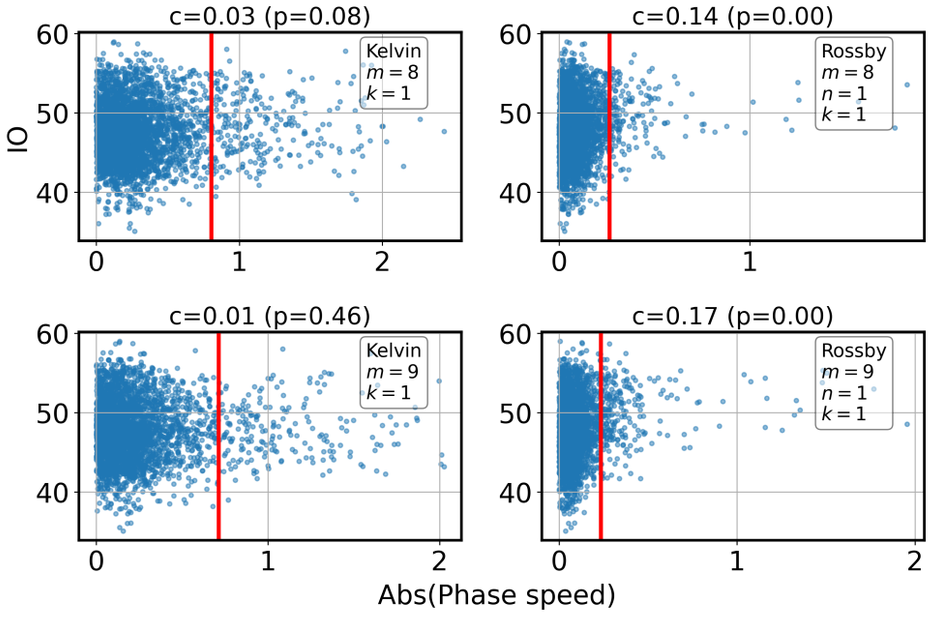


FIG. 8. Scatter diagrams between the total column water vapor (TCWV) over the equatorial Indian Ocean (IO; $10^{\circ}S$ - $10^{\circ}N$ and 60°E - 100°E) sector and the instantaneous frequencies $\tilde{\omega}^{(\alpha)}_{m,k,n}(t)$ of Kelvin (left panels) and Rossby (right panels) modes that mostly contribute to the tropical variability of the MJO. The zonal wavenumber $k$, the vertical mode index $m$, and the meridional quantum number $n$ are displayed at each panel. The respective correlations and p-values are displayed at the top of each panel. The corresponding eigenfrequency predicted by dry linear theory for each normal mode is illustrated as a red line. All the points refer to active MJO days ($|OMI| > 1.5$)

Next, inspired by the nonlinear theories of the MJO[38–42], we investigate the dependencies of the normal modes' instantaneous frequencies on their amplitudes. The results are displayed in Figure 11, showing in all cases a strong and statistically significant negative correlation between

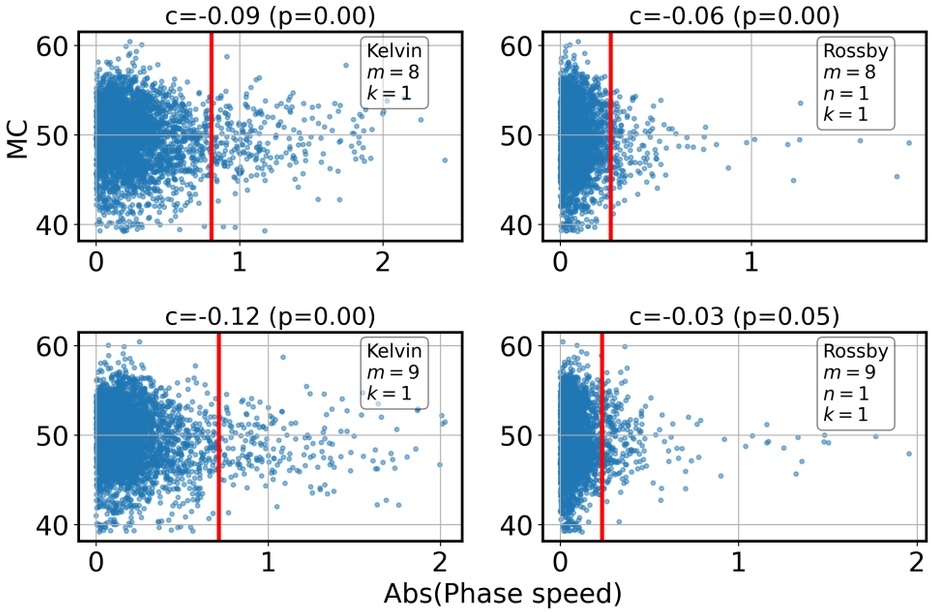


FIG. 9. Similar to Fig. 8, but for the TCWV over the equatorial maritime continent (MC; 10°S - 10°N and 100°E - 140°E) sector.

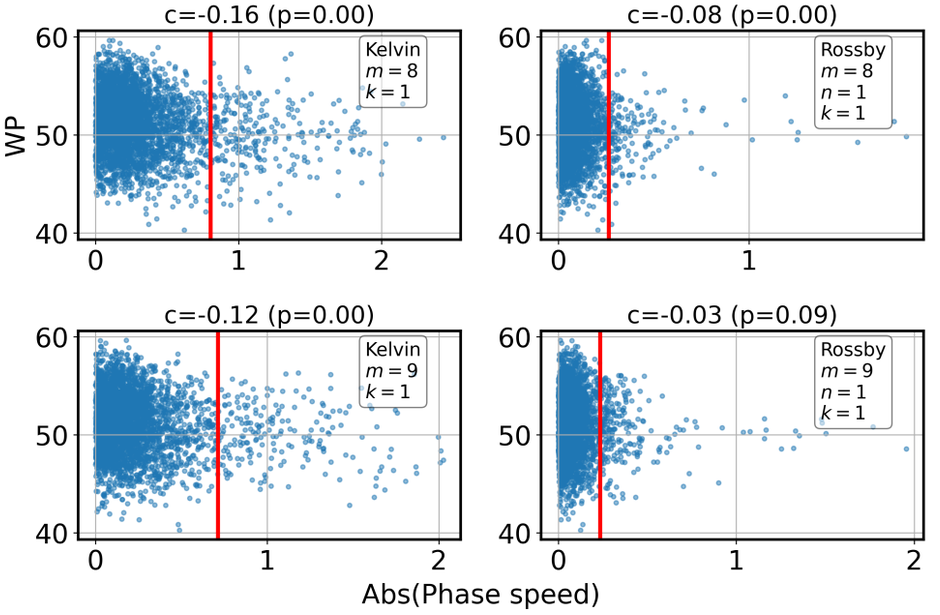


FIG. 10. Similar to Fig. 8, but for the TCWV over the equatorial Western Pacific (WP; 10°S - 10°N and 140°E - 180°) sector.

the instantaneous frequency and the amplitude of the normal modes ($-0.45 < c < -0.42$). This suggests that nonlinearity plays a central role in controlling the propagation of global-scale Kelvin and Rossby waves in the MJO package. The distribution of points in the scatter diagrams displayed in Fig. 11 suggests that applying a transformation $y = log(A)$ provides a linear relationship between the variables; these results are presented in the supplementary material.

## VII. DISCUSSION

In this study, we have explored the dynamics of global-scale atmospheric normal modes, primarily contributing to the tropical variability of the Madden-Julian Oscillation. Specifically, we focused on the zonal wavenumber-1 Rossby and Kelvin waves, both exhibiting a vertical structure compatible with the tropical circulation response to deep convection heating. The amplitudes and phases of these wave modes have been obtained through normal mode projection of ERA-5 reanalysis data onto the basis set provided by the eigensolutions of the *primitive equations linearized around a resting background state.* In particular, we have examined the role of moisture on the amplitudes and instantaneous frequencies of these wave modes. Additionally, to analyze the impact of nonlinearity on the propagation of these wave modes, we have investigated the relationship between their amplitudes and instantaneous frequencies.

Our findings suggest that moisture plays a role in driving these waves in active MJO cases and exhibits a moderate correlation with the instantaneous frequencies of these waves. A high and statistically significant negative correlation was found between the amplitudes of global-scale Rossby and Kelvin waves and their corresponding instantaneous frequencies, indicating that nonlinearity indeed plays a role in the propagation of these planetary-scale MJO-related normal modes.

Indeed, the dependence of the propagation speed of the wave on its amplitude is a common feature in nonlinear wave models. For example, an amplitude-dependent propagation has been reported in triads of Rossby-Haurwitz waves[49], as well as in solitons involving equatorial atmospheric waves[50,51]. Specifically, in the context of the MJO, the nonlinearity plays a central role in the propagation of equatorial modons that have been proposed as a mechanism for the MJO[38–42]. Recently, an evidence for the role of nonlinearity on the MJO propagation was also found in observations. For instance, by applying the SINDy technique for the analysis of MJO indices, Diaz, Barreiro, and Rubido[46] found a distinction between MJO events during El-Niño and La Niña years, showing that the events occurring during El-Niño years exhibited increased complexity,

nonlinearity and slower propagation.

In this study, we applied the SINDy technique to the amplitude variables of the planetary-scale Rossby and Kelvin waves, along with a moisture variable measuring the total column water vapor in the Maritime Continent and Western Pacific regions. The resulting model equations revealed the role of moisture in exciting the global-scale Rossby and Kelvin modes through a linear instability in the Kelvin wave, which is enhanced by increasing the moisture variable. Additionally, a parametric linear interaction between the Rossby and Kelvin modes was identified. This cross-linear interaction between Rossby and Kelvin waves through the moisture variable might be akin to the wave interaction mechanism involving an inertio-gravity mode and a Rossby mode through resonance with the diurnal cycle of the background moisture field in the context of a deep convection parameterization studied by Raupp and Silva Dias [80]. According to this theoretical study, the dynamics of this interaction is strongly dependent upon the latitude of the forcing. This suggests that the time-dependent part of the moisture filed involved in the energy transference from Kelvin to Rossby modes verified in our SINDy analysis might undergo a significant seasonal variation. In fact, Lu and Hsu [92] found that the low-level moisture field is a key factor for the seasonal variations in the MJO strength. Therefore, the approach adopted here to analyze the relationship between the amplitudes and phases of the MJO related waves as well as their relationship with the moisture field could be applied for the time-series referred to separate seasons rather than all the year round in order to investigate the seasonal variation of these MJO-related normal modes. We intend to investigate this point in a future work.

Therefore, our results suggest that nonlinearity plays a role in the propagation of the planetary-scale structure associated with the MJO. Recently, Mayta and Adames-Corraliza [43] suggested that the MJO behaves as a moisture mode at the synoptic-scale (zonal wave-numbers $3 \leq k \leq 6$), but likely not at the global-scale ($k \leq 2$). Integrating our findings with the conclusions of Mayta and Adames-Corraliza [43], it can be conjectured that the MJO propagation is predominantly governed by moisture at the synoptic-scale and by nonlinearity at the global-scale, with the moisture field playing the role of exciting or enhancing the amplitudes of these normal modes. In the present study, the role of synoptic-scale waves has been omitted. However, a thorough analysis of the interaction between synoptic and global-scale wave modes contributing to the Madden-Julian Oscillation should offer insights into questions regarding the MJO dynamics, such as how the selection of MJO's spatial scales occurs[93] and what drives different types of MJO propagation regimes[94,95].

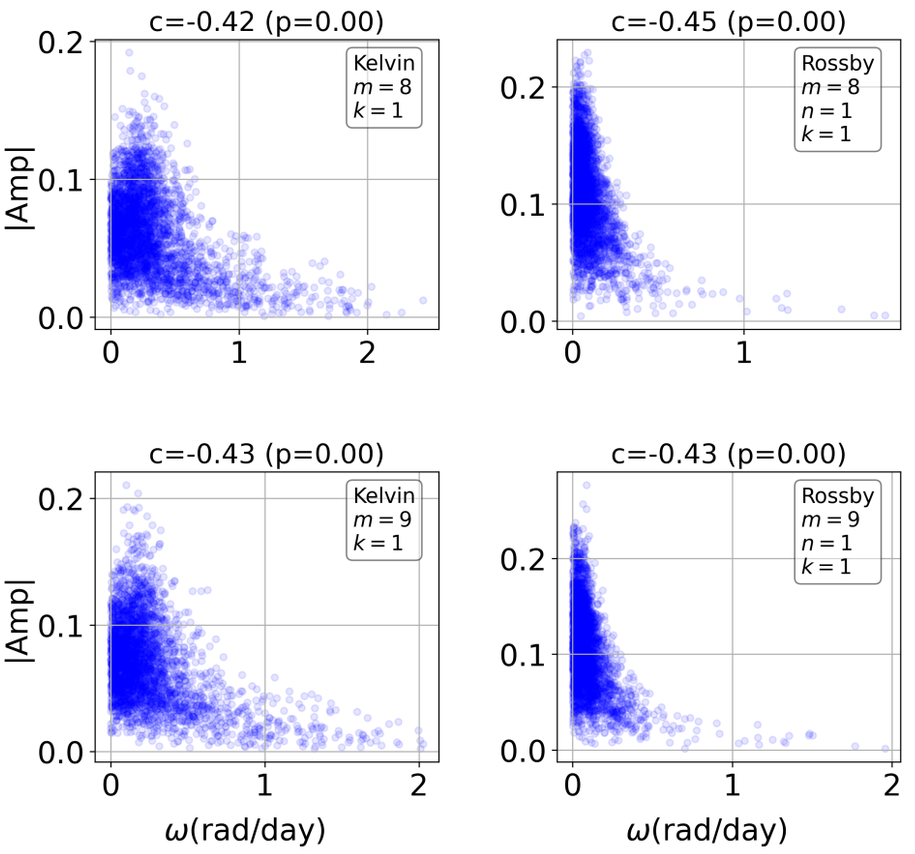


FIG. 11. Scatter diagrams between the instantaneous frequency $\tilde{\omega}^{(\alpha)}_{m,k,n}(t)$ and amplitude $|\chi^{(\alpha)}_{m,k,n}|(t)$ of the normal modes that mostly contribute to the tropical variability of the MJO; their zonal wavenumbers k, meridional indices n and vertical mode indices m are displayed at each panel. The respective correlations and p-values are displayed at the top of each panel. All the points refer to active MJO days ($|OMI| > 1.5$)

## SUPPLEMENTARY MATERIAL

In the supplementary material, we include a Figure (Figure 1 of the supplementary material) with the distribution (histogram) of the SINDy coefficients associated with equation 20 resulting from the ensemble analysis. Figure 2 of the supplementary material is an alternative version of Fig. 11 with a logaritmic transformation applied to the dataset, highlighting the amplitude-velocity correlation.

## ACKNOWLEDGMENTS

The work reported here has been supported by Fundação de Amparo à Pesquisa do Estado de São Paulo (FAPESP) (grants 2015/50122-0 and 2020/14162-6) and Coordenação de Aperfeiçoamento de Pessoal de Nível Superior - Brasil (CAPES) - Finance Code 001. BR acknowledges support from the National Center for Atmospheric Research, which is a major facility sponsored by the National Science Foundation under cooperative agreement 1852977, and also acknowledges partial support from NASA grants, such as NASA-LWS award 80NSSC20K0355 (awarded to NCAR) and NASA-HSR award 80NSSC21K1676 (awarded to NCAR). The authors are thankful to Dr. Juliana Dias for the helpful suggestions that improved this manuscript.

## DATA AVAILABILITY STATEMENT

The datasets used here were obtained from the ECMWF website at https://www.ecmwf.int/. The time-series of the normal mode spectral amplitudes are available at https://doi.org/10.5281/zenodo.4437766.

## REFERENCES

[1]A. Timmermann, S.-I. An, J.-S. Kug, F.-F. Jin, W. Cai, A. Capotondi, K. M. Cobb, M. Lengaigne, M. J. McPhaden, M. F. Stuecker, *et al.*, "El niño–southern oscillation complexity," Nature **559**, 535–545 (2018).

[2]C. Zhang, "Madden-Julian oscillation," Reviews of Geophysics **43** (2005).

[3]M. Baldwin, L. Gray, T. Dunkerton, K. Hamilton, P. Haynes, W. Randel, J. Holton, M. Alexander, I. Hirota, T. Horinouchi, *et al.*, "The quasi-biennial oscillation," Reviews of Geophysics **39**, 179–229 (2001).

[4]P. Delplace, J. Marston, and A. Venaille, "Topological origin of equatorial waves," Science **358**, 1075–1077 (2017).

[5]K. A. Emanuel, "An air-sea interaction model of intraseasonal oscillations in the tropics," Journal of Atmospheric Sciences **44**, 2324–2340 (1987).

[6]G. N. Kiladis, M. C. Wheeler, P. T. Haertel, K. H. Straub, and P. E. Roundy, "Convectively coupled equatorial waves," Reviews of Geophysics **47** (2009).

[7]R. S. Lindzen, "Wave-CISK in the tropics," Journal of Atmospheric Sciences **31**, 156–179 (1974).

[8]E. Ramirez, P. L. da Silva Dias, and C. F. Raupp, "Multiscale atmosphere–ocean interactions and the low-frequency variability in the equatorial region," Journal of the Atmospheric Sciences **74**, 2503–2523 (2017).

[9]A. J. Majda and J. A. Biello, "The nonlinear interaction of barotropic and equatorial baroclinic Rossby waves," Journal of the atmospheric sciences **60**, 1809–1821 (2003).

[10]C. F. Raupp, P. L. S. Dias, E. G. Tabak, and P. Milewski, "Resonant wave interactions in the equatorial waveguide," Journal of the atmospheric sciences **65**, 3398–3418 (2008).

[11]C. F. Raupp and P. L. S. Dias, "Resonant wave interactions in the presence of a diurnally varying heat source," Journal of the Atmospheric Sciences **66**, 3165–3183 (2009).

[12]B. Khouider, A. J. Majda, and S. N. Stechmann, "Climate science in the tropics: waves, vortices and PDEs," Nonlinearity **26**, R1 (2012).

[13]T. Matsuno, "Quasi-geostrophic motions in the equatorial area," Journal of the Meteorological Society of Japan. Ser. II **44**, 25–43 (1966).

[14]A. E. Gill, "Some simple solutions for heat-induced tropical circulation," Quartely Journal of the Royal Meteorological Society **106**, 447–462 (1980).

[15]M. Yanai and T. Maruyama, "Stratospheric wave disturbances propagating over the equatorial Pacific," Journal of the Meteorological Society of Japan. Ser. II **44**, 291–294 (1966).

[16]M. Wheeler and G. N. Kiladis, "Convectively coupled equatorial waves: Analysis of clouds and temperature in the wavenumber–frequency domain," Journal of the Atmospheric Sciences **56**, 374–399 (1999).

[17]T. Tsuda, Y. Murayama, H. Wiryosumarto, S. W. B. Harijono, and S. Kato, "Radiosonde observations of equatorial atmosphere dynamics over indonesia: 1. equatorial waves and diurnal tides," Journal of Geophysical Research: Atmospheres **99**, 10491–10505 (1994).

[18]J. W. Bergman and M. L. Salby, "Equatorial wave activity derived from fluctuations in observed convection," Journal of the atmospheric sciences **51**, 3791–3806 (1994).

[19]A. H. Sobel, J. Nilsson, and L. M. Polvani, "The weak temperature gradient approximation and balanced tropical moisture waves," Journal of the Atmospheric Sciences **58**, 3650 – 3665 (2001).

[20]D. J. Raymond and Ž. Fuchs, "Moisture modes and the Madden–Julian oscillation," Journal of Climate **22**, 3031–3046 (2009).

[21]Á. F. Adames and D. Kim, "The MJO as a Dispersive, Convectively Coupled Moisture Wave: Theory and Observations," Journal of the Atmospheric Sciences **73**, 913 – 941 (2016).

[22]Z. Fuchs-Stone, D. J. Raymond, and S. Sentic, "A simple model of convectively coupled equatorial Rossby waves," Journal of Advances in Modeling Earth Systems **11**, 173–184 (2018).

[23]A. Sobel and E. Maloney, "Moisture modes and the eastward propagation of the MJO," Journal of the Atmospheric Sciences **70**, 187–192 (2013).

[24]A. J. Majda and S. N. Stechmann, "The skeleton of tropical intraseasonal oscillations," Proceedings of the National Academy of Sciences **106**, 8417–8422 (2009).

[25]A. J. Majda and S. N. Stechmann, "Nonlinear dynamics and regional variations in the MJO skeleton," Journal of the Atmospheric Sciences **68**, 3053–3071 (2011).

[26]Á. F. Adames and D. Kim, "The MJO as a dispersive, convectively coupled moisture wave: Theory and observations," Journal of the Atmospheric Sciences **73**, 913–941 (2016).

[27]B. Khouider and A. J. Majda, "A simple multicloud parameterization for convectively coupled tropical waves. part I: linear analysis," Journal of the Atmospheric Sciences **63**, 1308–1323 (2006).

[28]B. Khouider and A. J. Majda, "A simple multicloud parameterization for convectively coupled tropical waves. part II: nonlinear simulations," Journal of the Atmospheric Sciences **64**, 381–400 (2007).

[29]B. Khouider and A. J. Majda, "Multicloud models for organized tropical convection: enhanced congestus heating," Journal of the Atmospheric Sciences **65**, 895–914 (2008).

[30]R. A. Madden and P. R. Julian, "Observations of the 40–50-day tropical oscillation — A review," Monthly weather review **122**, 814–837 (1994).

[31]A. M. Grimm, "Madden–Julian Oscillation impacts on South American summer monsoon season: precipitation anomalies, extreme events, teleconnections, and role in the MJO cycle," Climate Dynamics **53**, 907–932 (2019).

[32]C. Jones, D. E. Waliser, K. Lau, and W. Stern, "The Madden–Julian oscillation and its impact on northern hemisphere weather predictability," Monthly weather review **132**, 1462–1471 (2004).

[33]S. Singh, R. Kripalani, and D. Sikka, "Interannual variability of the Madden–Julian oscillations in indian summer monsoon rainfall," Journal of Climate , 973–978 (1992).

[34]A. E. Gill, *Atmosphere-ocean dynamics*, Vol. 30 (Academic press, 1982).

[35]C. Zhang, Á. Adames, B. Khouider, B. Wang, and D. Yang, "Four theories of the Madden-Julian oscillation," Reviews of Geophysics **58**, e2019RG000685 (2020).

[36]J. D. Neelin and J.-Y. Yu, "Modes of tropical variability under convective adjustment and the Madden-Julian oscillation. Part I: Analytical results." J. Atmos. Sci. **51**, 1876–1894 (1994).

[37]C. Zhang, Á. F. Adames, B. Khouider, B. Wang, and D. Yang, "Four theories of the madden-julian oscillation," Reviews of Geophysics **58**, e2019RG000685 (2020).

[38]J.-I. Yano and J. J. Tribbia, "Tropical atmospheric Madden–Julian oscillation: A strongly nonlinear free solitary Rossby wave?" Journal of the Atmospheric Sciences **74**, 3473–3489 (2017).

[39]M. Rostami and V. Zeitlin, "Eastward-moving convection-enhanced modons in shallow water in the equatorial tangent plane," Physics of Fluids **31** (2019).

[40]M. Rostami and V. Zeitlin, "Eastward-moving equatorial modons in moist-convective shallow-water models," Geophysical & Astrophysical Fluid Dynamics **115**, 345–367 (2021).

[41]M. Rostami and V. Zeitlin, "Can geostrophic adjustment of baroclinic disturbances in the tropical atmosphere explain MJO events?" Quarterly Journal of the Royal Meteorological Society **146**, 3998–4013 (2020).

[42]M. Rostami and V. Zeitlin, "On the genesis and dynamics of Madden–Julian oscillation-like structure formed by equatorial adjustment of localized heating," Quarterly Journal of the Royal Meteorological Society **148**, 3788–3813 (2022).

[43]V. C. Mayta and Á. F. Adames-Corraliza, "Is the Madden-Julian Oscillation a moisture mode?" Geophysical Research Letters , e2023GL103002 (2023).

[44]M. C. Wheeler and H. H. Hendon, "An all-season real-time multivariate MJO index: Development of an index for monitoring and prediction," Monthly weather review **132**, 1917–1932 (2004).

[45]G. N. Kiladis, J. Dias, K. H. Straub, M. C. Wheeler, S. N. Tulich, K. Kikuchi, K. M. Weickmann, and M. J. Ventrice, "A comparison of OLR and circulation-based indices for tracking the MJO," Monthly Weather Review **142**, 1697–1715 (2014).

[46]N. Diaz, M. Barreiro, and N. Rubido, "Data driven models of the Madden-Julian Oscillation: understanding its evolution and ENSO modulation," Climate and Atmospheric Science **6** (2023).

[47]N. Žagar and C. L. Franzke, "Systematic decomposition of the Madden-Julian oscillation into balanced and inertio-gravity components," Geophysical Research Letters **42**, 6829–6835 (2015).

[48]A. Majda, *Introduction to PDEs and Waves for the Atmosphere and Ocean*, Vol. 9 (American Mathematical Soc., 2003).

[49]B. Raphaldini, P. d. S. Peixoto, A. S. W. Teruya, C. F. M. Raupp, and M. D. Bustamante, "Precession resonance of Rossby wave triads and the generation of low-frequency atmospheric oscillations," Physics of Fluids **34** (2022).

[50]J. P. Boyd, "Equatorial solitary waves. part I: Rossby solitons," Journal of Physical Oceanography **10**, 1699–1717 (1980).

[51]J. P. Boyd, "Equatorial solitary waves. part II: Envelope solitons," Journal of Physical Oceanography **13**, 428–449 (1983).

[52]J. J. Tribbia, "Modons in spherical geometry," Geophysical & Astrophysical Fluid Dynamics **30**, 131–168 (1984).

[53]A. D. Craik, *Wave interactions and fluid flows* (Cambridge University Press, 1988).

[54]A. S. Teruya, B. Raphaldini, V. C. Mayta, C. F. Raupp, and P. L. da Silva Dias, "Wavenumber-frequency spectra of normal mode function decomposed atmospheric data: Departures from the dry linear theory," Atmosphere **14**, 622 (2023).

[55]A. Kasahara and K. Puri, "Spectral representation of three-dimensional global data by expansion in normal mode functions," Monthly Weather Review **109**, 37–51 (1981).

[56]G. I. Taylor, "The oscillations of the atmosphere," Procedings of the Royal Society of London **156**, 318–326 (1936).

[57]M. S. Longuet-Higgins, "The eigenfunctions of Laplace's tidal equation over a sphere," Philosophycal Transactions of the Royal Society A **262**, 511–607 (1968).

[58]A. Kasahara, "Normal modes of ultralong waves in the atmosphere," Monthly Weather Review **104**, 669–690 (1976).

[59]A. Kasahara, "Numerical integration of the global barotropic primitive equations with Hough harmonic expansions," Journal of the Atmospheric Sciences **34**, 687–701 (1977).

[60]N. Žagar, A. Kasahara, K. Terasaki, J. Tribbia, and H. Tanaka, "Normal-mode function representation of global 3-D data sets: open-access software for the atmospheric research community," Geoscientific Model Development **8**, 1169–1195 (2015).

[61]B. Raphaldini, A. S. Wakate Teruya, P. L. Silva Dias, V. R. Chavez Mayta, and V. J. Takara, "Normal mode perspective on the 2016 QBO disruption: Evidence for a basic state regime transition," Geophysical Research Letters **47**, e2020GL087274 (2020).

[62]B. Raphaldini, A. S. Teruya, P. Leite da Silva Dias, L. Massaroppe, and D. Y. Takahashi, "Stratospheric ozone and quasi-biennial oscillation (QBO) interaction with the tropical troposphere on intraseasonal and interannual timescales: a normal-mode perspective," Earth System Dynamics **12**, 83–101 (2021).

[63]M. J. Ventrice, M. C. Wheeler, H. H. Hendon, C. J. Schreck III, C. D. Thorncroft, and G. N. Kiladis, "A modified multivariate Madden–Julian oscillation index using velocity potential,"

Monthly Weather Review **141**, 4197–4210 (2013).

[64]B. J. Hoskins and D. J. Karoly, "The steady linear response of a spherical atmosphere to thermal and orographic forcing," Journal of the Atmospheric Sciences **38**, 1179–1196 (1981).

[65]D. J. Karoly, "Southern Hemisphere circulation features associated with El Niño-southern oscillation," Journal of Climate **2**, 1239–1252 (1989).

[66]K. C. Mo and R. W. Higgins, "The Pacific-South American modes and tropical convection during the southern hemisphere winter," Monthly Weather Review **126**, 1581–1596 (1998).

[67]H. Lim and C.-P. Chang, "Generation of internal-and external-mode motions from internal heating: Effects of vertical shear and damping," Journal of the Atmospheric Sciences **43**, 948–960 (1986).

[68]A. Kasahara and P. L. Silva Dias, "Response of planetary waves to stationary tropical heating in a global atmosphere with meridional and vertical shear," Journal of the Atmospheric Sciences **43**, 1893–1911 (1986).

[69]B. Wang and X. Xie, "Low-frequency equatorial waves in vertically sheared zonal flow. part I: stable waves," Journal of the Atmospheric Sciences **53**, 449–467 (1996).

[70]J. Ferguson, B. Khouider, and M. Namazi, "Two-way interactions between equatorially-trapped waves and the barotropic flow," Chinese Annals of Mathematics **30B**, 539–568 (2009).

[71]D. Wang, J. Yano, and Y. Lin, "Madden–julian oscillations seen in the upper-troposphere vorticity field: Interactions with rossby wave trains," Journal of Atmospheric Sciences **76**, 1785–1807 (2019).

[72]S. L. Brunton, J. L. Proctor, and J. N. Kutz, "Discovering governing equations from data by sparse identification of nonlinear dynamical systems," Proceedings of the national academy of sciences **113**, 3932–3937 (2016).

[73]V. Mayta and A. F. Adames Corraliza, "The stirring tropics: the ubiquity of moisture modes and moisture-vortex instability," Journal of Climate **37**, 1981–1997 (2024).

[74]J. A. Biello and A. J. Majda, "A new multiscale model for the Madden–Julian Oscillation," Journal of the Atmospheric Sciences **62**, 1694–1721 (2005).

[75]M. Roxy, P. Dasgupta, M. J. McPhaden, T. Suematsu, C. Zhang, and D. Kim, "Twofold expansion of the Indo-Pacific warm pool warps the MJO life cycle," Nature **575**, 647–651 (2019).

[76]D. J. Raymond and Ž. Fuchs, "The Madden-Julian oscillation and the Indo-Pacific warm pool," Journal of Advances in Modeling Earth Systems **10**, 951–960 (2018).

[77]P. E. Roundy, "Analysis of convectively coupled kelvin waves in the indian ocean mjo," Journal of the Atmospheric Sciences **66**, 3165–3183 (2008).

[78]B. Raphaldini, A. Teruya, C. Raupp, P. Silva-Dias, and D. Takahashi, "Information flow between MJO-related waves: a network approach on the wave space," The European Physical Journal Special Topics **230**, 3009–3017 (2021).

[79]B. M. de Silva, K. Champion, M. Quade, J.-C. Loiseau, J. N. Kutz, and S. L. Brunton, "Pysindy: a python package for the sparse identification of nonlinear dynamics from data," arXiv preprint arXiv:2004.08424 (2020).

[80]C. F. M. Raupp and P. L. Silva Dias, "Interaction of equatorial waves through resonance with the diurnal cycle of tropical heating," Tellus A **62**, 706–718 (2010).

[81]Y. Hayashi, "A theory of large-scale equatorial waves generated by condensational heat and accelerating the zonal wind," Journal of Meteorological Society of Japan **48**, 140–160 (1970).

[82]D. E. Stevens and R. S. Lindzen, "Tropical wave-cisk with a moisture budget and cumulus friction," Journal of the Atmospheric Sciences **35**, 940–961 (1978).

[83]D. Ciro, B. Raphaldini, and C. F. M. Raupp, "Topography-induced locking of drifting Rossby–Haurwitz waves," Physics of Fluids **32** (2020).

[84]A. J. Majda, R. Rosales, E. G. Tabak, and C. Turner, "Interaction of large-scale equatorial waves and dispersion of kelvin waves through topographic resonances," Journal of the Atmospheric Sciences **56**, 4118–4133 (1999).

[85]C. Zhang and M. Dong, "Seasonality in the Madden–Julian oscillation," Journal of climate **17**, 3169–3180 (2004).

[86]C.-P. Chang and H. Lim., "Kelvin wave-CISK: a possible mechanism for the 30-50 day oscillations," Journal of the Atmospheric Sciences **45**, 1709–1720 (1988).

[87]K.-M. Lau and L. Peng, "Origin of low-frequency (intraseasonal) oscillations in the tropical atmosphere. part I: Basic theory," Journal of the Atmospheric Sciences **44**, 950–972 (1987).

[88]B. Wang and H. Rui, "Dynamics of the coupled moist Kelvin-Rossby wave on an equatorial beta-plane," Journal of the Atmospheric Sciences **47**, 397–413 (1990).

[89]Z. Fuchs and D. J. Raymond, "A simple model of intraseasonal oscillations," Journal of Advances in Modeling Earth Systems **9**, 1195–1211 (2017).

[90]P. L. Silva Dias, W. H. Schubert, and M. DeMaria, "Large-scale response of the tropical atmosphere to transient convection," Journal of the Atmospheric Sciences **40**, 2689–2707 (1983).

[91]M. Rostami and V. Zeitlin, "Geostrophic adjustment on the equatorial Beta-plane revisited." Physicas of Fluids **31**, 081702 (2019).

[92]W. Lu and P.-C. Hsu, "Factors controlling the seasonality of the madden-julian oscillation," Dynamics of Atmospheres and Oceans **78**, 106–120 (2017).

[93]F. Ahmed, "The MJO on the equatorial beta plane: An eastward-propagating Rossby wave induced by meridional moisture advection," Journal of the Atmospheric Sciences **78**, 3115–3135 (2021).

[94]D. Kim, J.-S. Kug, and A. H. Sobel, "Propagating versus nonpropagating Madden–Julian oscillation events," Journal of Climate **27**, 111–125 (2014).

[95]D. Kim, H. Kim, and M.-I. Lee, "Why does the MJO detour the maritime continent during austral summer?" Geophysical Research Letters **44**, 2579–2587 (2017).

[96]S. L. Brunton and J. N. Kutz, *Data-driven science and engineering: Machine learning, dynamical systems, and control* (Cambridge University Press, 2022).

[97]U. Fasel, J. N. Kutz, B. W. Brunton, and S. L. Brunton, "Ensemble-sindy: Robust sparse model discovery in the low-data, high-noise limit, with active learning and control," Proceedings of the Royal Society A **478**, 20210904 (2022).

[98]J. D. Neelin, I. M. Held, and K. H. Cook, "Evaporation-wind feedback and low-frequency variability in the tropical atmosphere," Journal of Atmospheric Sciences **44**, 2341–2348 (1987).